

THE TESTING OF A PASSIVE SOLAR WINDOW HEATER

R.P. Kirchner, Ph.D., P.E. J.J. Garfall

ABSTRACT

A passive solar window heater for supplementary space heating was designed, constructed, and tested. This flat-plate passive collector was constructed by covering a wooden frame with a dimpled, black chrome plated absorber sheet. Six rear air passages insulated on the room side provided a 5 foot vertical solar-heated chimney. The 6 ft x 8 ft window heater was installed in a south-oriented window, and experimental data were taken during summer and winter conditions. Instrumentation was provided to measure and record temperatures, solar insolation, and air velocities. Useful heat gains were determined and provided operational data for mathematical model verification and the development of simplified design procedures and recommendations.

INTRODUCTION

Through proper design, windows can significantly reduce the cost of the energy needed to maintain building comfort. By considering window siting, exterior and interior additions, framing, glazing, and room interior, a number of opportunities exist for making windows more energy efficient (Hastings and Crenshaw 1977; Shurcliff 1980). Interior additions would include such items as opaque shades and blinds, curtains and draperies, special film shades (e.g., transparent, reflective, absorbing), and solar window heaters/insulating shutters. In this paper, a passive solar window heater for supplementary space heating and year-round window insulation was designed, constructed, and tested during both summer and winter conditions. While the present design provided a fixed indoor window cover, a swinging shutter design would retain all normal window functions and use. These would include solar gains when desired, daylighting, shading, insulation (noise and thermal), airtightness, and ventilation, as well as such items as view and aesthetic considerations and emergency exit.

The passive window heater uses a simple wood-frame structure covered on the indoor glass side with a selective absorber and covered on the room side with a rigid insulation board with protective covering (i.e., fireproof covering for insulation). A data-logging system was used to measure and record eight temperatures, solar insolation, entrance velocity, and time. From these measurements, the useful heat gain could be determined. These experimental results provide a baseline of thermal performance for the testing and verification of a suitable mathematical model and the development of a simplified design chart.

R. P. Kirchner , Associate Professor of Mechanical Engineering, New Jersey Institute of Technology, Newark, N.J., and J. J. Garfall , Senior Engineer, Singer Co., Singer Electronic Systems Div., Totowa, N.J.

While the primary goal of this paper is to present these experimental test results and simple thermal design recommendations, the preliminary results of a thermal model are also presented and compared with experimental evidence. Simplified design curves are presented, which will reduce the effort required by an architect, engineer, or contractor-builder called upon to provide an effective thermal design. The thermal design procedure is simple and straightforward in application and is based on established solar engineering principles (Duffie and Beckman 1980).

This paper focuses on the thermal design of a passive solar window heater and is not an effort to produce a prototype for commercialization or to produce self-installation plans. This would require additional design considerations including materials compatibility, materials out-gassing, temperature limitations, differential expansion, longevity, and fire and building code compliance. Building code considerations would require the covering of rigid insulations with noncombustible material and coverings or substitute materials for the wood frame in contact with the absorber sheet.

The short-term transient thermal behavior of the window heater was also determined for a step increase and decrease in solar radiation. From these results a time constant was determined and was found to be on the order of one to two minutes for the start of useful heat delivery.

DESIGN AND CONSTRUCTION

The passive solar window heater (see Figure 1) is a flatplate-type collector constructed by covering a wood frame with a selectively coated copper absorber sheet. The existing single-pane window provided the glazing for the collector. Vertical 2 by 4s serve as dividers for six flow passages. The flow passages behind the absorber sheet were insulated with foilfaced one-inch-thick rigid insulation material (R7 per inch). The insulation was covered on the room side with 0.50 in (0.013 m) plywood. The lower portion of the collector frame was not covered with an absorber sheet or insulation. Instead, two hinged windows were provided to permit window access and admit natural light. When closed, these lower windows would create a double-glazed system. The upper fixed collector and lower window design were necessary due to the heavy frame and lack of side space for shutter storage. Future designs would be constructed with a considerably lighter frame with no lower inside window and fully hinged. In this way, they could be opened (or removed) when not in use or closed to prevent losses (or gains). For the most part, normal window functions were retained.

The copper absorber sheet has a black chrome selective surface. This surface was textured (dimpled) to provide 14% more surface area, add rigidity to the thin copper sheet (.005 in [0.13 mm]), and enhance conditions for turbulent flow. The black chrome on nickel-plated copper strip has an average solar absorptance of 0.95 ± 0.02 and an infrared emittance of 0.10 ± 0.02 at room temperature (Lampert 1979). The finished absorber sheet is provided with a clear polymer sheet, which protects the sheet from abrasion and contamination (e.g., hand prints) during handling. The quick-release coating is easily removed after fastening. Absorber strips 12 in (0.305 m) wide were overlapped to form vertical 11 in (0.28 m) centers and were secured by 0.50 in (0.013 m) aluminum batten strips screwed to the wooden frame. The absorber sheet was curved to a 3.5 in (0.089 m) radius at the top to form a wall guide vane at the return duct opening, as shown in Figure 1. While not detailed in Figure 1, the thermosiphon heater would be fitted with a back-flow damper to prevent reverse circulation at night.

Sealing where necessary, to prevent flow leakage and reduce infiltration, was provided by RTV silicon seal caulking. The existing opaque window shade between the glazing and the absorber sheet was used to start or stop solar insolation to the absorber. In this way it served as an on-off switch for the collector and provided additional dead air insulation space for winter night insulation. A slightly thicker window quilt could serve the same purpose and provide more insulation value; however, in view of the low

infrared emittance of the absorber sheet and additional cost factors, it may not be practical. The low infrared emittance is an important consideration, not only in improving collector performance, but also in reducing winter night radiation losses. The reduction in radiation and convective/conductive losses helps to increase human comfort near windows, since less body heat is radiated to the warmer inside surface than to a single-pane cold window.

Most thermosiphon systems utilize some form of heat storage. The passive solar window heater itself has insignificant thermal storage. It used the mass of the existing brick walls and concrete floors and ceilings, and room furnishings for thermal storage. The low thermal mass of the collector itself provides quick heat pickup, particularly on cloudy days. The short-term performance is discussed in detail in the section on transient response.

The collector was installed in a second-story window, which faced 20° west of true south. This orientation, fixed by available window location, clearly tended to favor afternoon collection with low early morning heat pickup. A single-story structure to the south provided no solar shading due to height differences, although some shading did occur due to the wide aluminum frames and the sides of the recessed window frame (see Figure 2). The total material cost of the window heater (including the absorber price of \$1.60/ft²) was approximately \$230 or \$6.90/ft². However, this first collector was hand-built and was structurally overdesigned. In addition, it is not absolutely necessary to use a black chrome absorber sheet. This cost could be substantially reduced using a lighter frame and mass production techniques to a total material cost of about \$4 to \$5/ft².

EXPERIMENTAL RESULTS

Eight temperatures were measured using type T thermocouples (copper-constantan). A programmable data logger with built-in conversion tables for J, K, and T thermocouple types and electronic reference junction was used to record all temperature data. Ice point and steam point references were checked, and it was determined that temperatures were measured to the nearest 1/2 degree ($\pm 0.28^\circ\text{C}$, $\pm 0.5^\circ\text{F}$). Temperatures were measured at flow inlet, flow outlet, room, inside glass surface, outside, and on the absorber sheet at 0.25, 0.50, and 0.75 height as shown in Figure 1. The outside thermocouple was shielded from direct solar radiation, and all surface thermocouples were affixed to the surface with an epoxy glue containing fine copper filings for high thermal conductivity.

Total solar radiation (beam + diffuse + reflected) was measured using a calibrated pyranometer. Insolation was measured in the vertical collector surface, under the glass, at a location without shadows from cross-frame members. The pyranometer supplied with manufacturer's calibration was estimated to have an accuracy of about $\pm 5\%$.

The center velocity at the flow entrance was measured using a constant temperature hot-film anemometer. A special-design probe, which has temperature compensation, is fairly nondirectionally sensitive ($\pm 15^\circ$ yaw limits), and was specifically designed for low-velocity air measurements, was used (see Figure 3). The accurate measurement of the very low velocities normally encountered in free convective heat transfer necessitates the use of a hot-film anemometer system capable of measurement in the range of about 0.25 to 1.5 ft/s (0.076 to 0.46 m/s).

The anemometer probe was manufactured by sputtering a nickel film on optically polished 2.6 mm diameter quartz spheres. The two sensor spheres, one for velocity measurement and a second for temperature compensation, were mounted on a thin nylon stem embedded in a hypodermic needle. After reviewing some of the procedures for user calibration (e.g., Aydin and Leutheusser 1959) it was determined to use a probe calibrated by the manufacturer in the range of 0.0705 to 1.306 ft/s (0.0215 to 0.398 m/s).

The calibration curve (velocity versus voltage) was plotted and curve fitted using a linear function below 0.525 ft/s (0.16 m/s), with maximum

percent error over the entire range of $\pm 1.5\%$. With low flow velocities, below 0.525 ft/s (0.16 m/s), the estimated error in velocity measurement was about 10%. With velocities in the higher range above 0.525 ft/s (0.16 m/s), the estimated error was about .05 ft/sec (0.015 m/s).

A probe fixture was designed to permit three coordinate movements of the anemometer probe, as shown in Figure 4. The fixture also allows a $\pm 15^\circ$ yaw adjustment to attain probe parallelism with the flow. A locking device permitted the final probe alignment to be fixed for the duration of the experiments.

The data acquisition system recorded eight temperatures, normal insolation, inlet center velocity, and time. The data logger provided a hard copy output (electrostatic printer on aluminized paper) of all measured variables and time. Generally a warmup and settling period of 45 minutes to one hour was permitted for stabilization of the anemometer from cold start.

Data were recorded 12 times per hour over a 10:00 a.m. to 4:00 p.m. day. A data set for use in the mathematical model development was produced by averaging the variable's reading across a given time period when the value of insolation was fairly constant (less than 10% variation). This procedure produced a data base whose elements represented the performance of the window heater under as close to steady-state insolation conditions as possible. The original tabulated data sets for use in a computer model are given in Figure 5.

TRANSIENT RESPONSE

The short-term response of the passive solar window heater to a step decrease and increase in solar radiation was determined experimentally and is presented in Figure 6. The test was conducted by using the window shade as a switch for turning the insolation on or off, thus producing essentially a step input of solar radiation.

The test began with the collector in near steady-state operation at midday on a clear sunny January day. After ten minutes of steady operation, the shade was pulled down, blocking the collector; 25 minutes later the shade was pulled up to admit radiation, and the collector was monitored for another 25 minutes. The record of the variation of absorber and outlet temperature with time provided a temperature-time history of the transient response to a step decrease and increase in solar radiation.

The standard time constant (i.e., time for 63.2% of the total change) for the step changes was found to be an average of 1.3 minutes for the absorber plate temperature and 2.1 minutes for the flow outlet temperature. These values, typical of air solar collectors, are quite low and verify that the collector has a low heat capacity (due to low mass). From cold start the collector reaches at least 95% of its steady-state thermal output within a time period of about six minutes. The absorber sheet itself reaches 95% of its final steady state temperature in about four minutes.

The quick heat pickup is useful on cloudy days when short periods (15 min) of sun appear, followed by longer cloudy periods.

DISCUSSION OF RESULTS

A steady-state¹ thermal model shown in Figure 7 was used to describe the behavior of the passive solar window heater. A general outline describing the calculation procedure is given below.

¹ The behavior of the collector is described by a quasi-steady model. It describes a process in which things vary so slowly in time that it can be approximated as a series of different steady state conditions.

The resistances R_1 through R_{12} were determined using empirical convective heat transfer coefficients, parallel plate and small gray-body-in-black-surroundings radiative conductances, and conduction thermal conductivities. The convective heat transfer coefficients between the insulation and the flowing air, between the absorber sheet and the flowing air, between the absorber sheet and the window glazing, and between the window glazing and the outside conditions were determined, based generally on preliminary calculated estimates. A relaxation technique was used to minimize the error and determine temperatures, such that the nodal current equations were satisfied (i.e., heat in = heat out for each node in steady state). The relaxation technique uses trial convective coefficients to calculate the prediction error in the useful heat gain and the flow outlet temperature. The set of trial coefficients that yielded, by trial and error, acceptable prediction errors and satisfied the steady-state nodal equation were taken to be the corrected coefficients. All of the coefficients were consistent with typical calculated values for natural convective film coefficients and ranged from 0.43 to 0.82 Btu/h·ft²·°F (2.44 to 4.66 W/m²·°C). Radiation resistances were not linearized, i.e., their values depended on the temperatures across the resistance.

A design chart (Figure 8) was developed that provides a simplified design procedure and requires a minimum of thermal engineering background. This chart will, for a specific collector geometry, permit the estimation of the thermal output if certain broad guidelines are followed. While presentations in dimensionless form convey considerable information and provide generality, a dimensional-specific case format is presented for ease of understanding. The design chart applies to passive collectors with a thermosiphon height of 5 to 6 ft (1.5 to 1.8 m), low thermal mass, a passage depth of approximately 3.5 in (0.09 m), and similar absorber sheet/insulation specifications.

Figure 8 shows a plot of collector output in Btu/h (W) versus insolation in Btu/h·ft² (W/m²) at various values of ΔT , here ΔT is the temperature difference between the room air and the outdoor air in °C. The constant ΔT curves were developed from the results of the mathematical model using the thermal circuit shown in Figure 7. This preliminary calculation used a constant average flow rate of 60 lb/h, typical of the passive heater performance under clear-day near-noon conditions.

Referring to Figure 8, if the designer needs to estimate the heat delivery for an outdoor temperature of 30°F (-1.1°C), an insolation of 60 Btu/h·ft² (189 W/m²), and a room temperature of 70°F (21.1°C); the value of ΔT is calculated, and, moving vertically from the insolation value (60) until intersecting the proper ΔT line 40°F (22.2°C), the output is given as 116 Btu/h (34 W) as shown in Figure 8. The amount of insolation, E_{in} , on a vertical surface on a given date for clear days is available for most latitudes. By successive application an hour-by-hour analysis could be made, and the average daily heat delivery could be approximated.

CONCLUSIONS

The experimental results provided a baseline of thermal performance data for the testing of the mathematical model and the production of a simplified thermal design chart.

One of the original objectives of this passive solar window heater was to provide a thermal shutter to cover a large old aluminum-framed retrofit window with considerable air leakage. The passive window heater would permit solar gains during the daytime, would significantly reduce cold air infiltration, and would reduce both day and night heat losses. This solar energy collecting, insulated window shutter can be an inexpensive alternative to complete window replacement, although the high infiltration on the original window can reduce the solar collection efficiency of this unit and produce conservative results in terms of the design chart. For a tightly fitted south-facing double-pane window (which already serves as a direct-gain solar

collector), a simple lower-cost insulating shutter could provide the same results.

The short-term transient behavior showed that a low heat capacity, passive window heater can provide quick heat pickup, even during short sun periods on cloudy days.

NOMENCLATURE²

E_{in} = Solar radiation absorbed by absorber sheet at T6 in Btu/h·ft² (W/m²).

Q_{out} = Useful heat gain in Btu/h·ft² (W/m²).

All resistances in h·ft²·°R/Btu (m² °K/W)

R_1 = Convective resistance between room air and inside of plywood facing.

R_2 = Resistance to heat flow by radiant heat transfer between the inside plywood facing and the room.

R_3 = Resistance to heat flow by conductive heat transfer through the room-side plywood facing.

R_4 = Resistance to heat flow at the interface of the plywood facing and the rigid insulation.

R_5 = Resistance to heat flow by conductive heat transfer through the 1-inch rigid insulation.

R_6 = Resistance to heat flow by convective heat transfer between the rigid insulation surface and the heated flowing air.

R_7 = Resistance to heat flow by convective heat transfer between the absorber sheet and the heated flowing air.

R_8 = Resistance to heat flow by radiant heat transfer between the absorber sheet and the rigid insulation.

R_9 = Resistance to heat flow by convective heat transfer between the absorber sheet and the window glass.

R_{10} = Resistance to heat flow by radiant heat transfer between the absorber sheet and the window glass.

R_{11} = Resistance to heat flow by convective heat transfer between the outside glass surface and the surroundings.

R_{12} = Resistance to heat flow by radiant heat transfer between the outside glass surface and the sky.

All measured temperatures in °F (°C).

T_0 = Room temperature.

T_1 = Inside surface temperature of plywood facing.

T_2 = Surface temperature of plywood side facing outside.

T_3 = Surface temperature of insulation side facing room.

² U.S. Customary Units given first with SI units given in parenthesis. Units used as recommended in Murdock (1977).

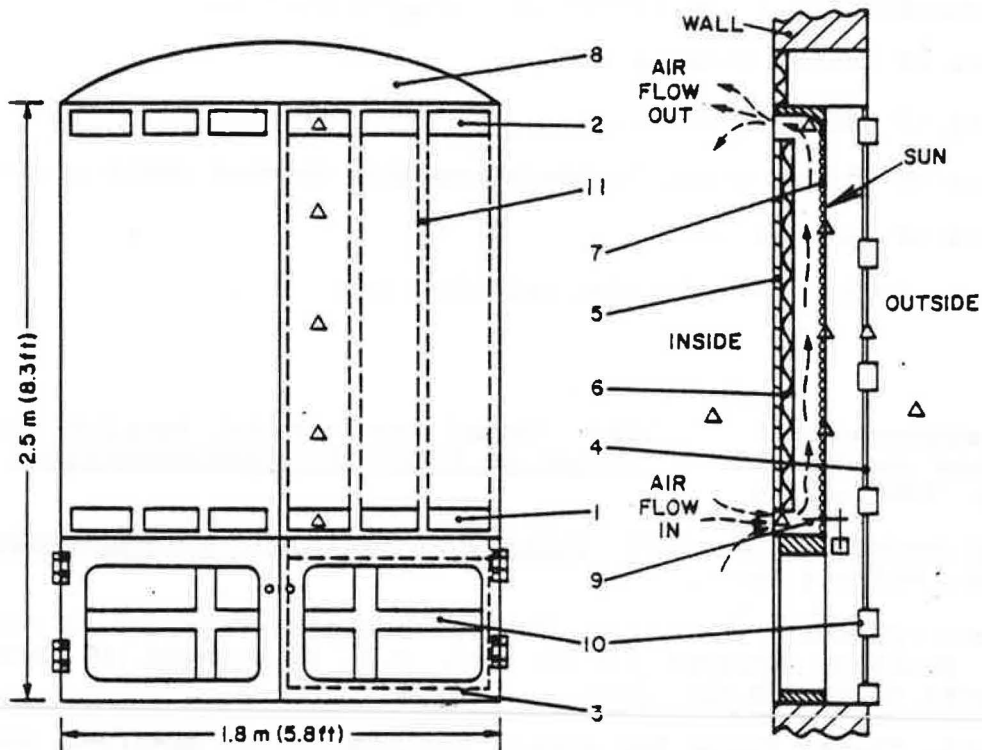
- T_4 = Surface temperature of insulation side facing outside.
 T_5 = Temperature of heated flowing air.
 T_6 = Temperature of absorber sheet.
 T_8 = Temperature of window glass (temperature drop through glass neglected).
 T_9 = Temperature of outside air.
 T_{sky} = Temperature of sky for radiation calculations.

REFERENCES

- Aydin, M., and Leutheusser, H. J. 1959. "Novel experimental facility for the study of plane couette flow." Review of Scientific Instrumentation, Vol. 50, Nov., pp. 1362 - 1366.
- Duffie, J.A., and Beckman, W.A. 1980. Solar engineering of thermal processes. New York: John Wiley & Sons.
- Hastings, S.R., and Crenshaw, R.W. 1977. "Window design strategies to conserve energy" NBS Building Science Series 104, U.S. Department of Commerce, National Bureau of Standards, June.
- Lampert, C.M. 1979. "Metal foils for direct application of absorber coatings on solar collectors." Lawrence Berkeley Laboratory, University of California, Materials and Molecular Research Division, August.
- Murdock, J.W. 1977. "SI units in heat transfer." ASME Text Booklet, 1st ed. The American Society of Mechanical Engineers, March.
- Shurcliff, W. 1980. Thermal shutters and shades. Andover, Mass: Brick House Publishing Co., Inc.

ACKNOWLEDGMENTS

The authors acknowledge and thank the New Jersey Institute of Technology for support of the research efforts on the passive solar window heater. Also, the encouragement and assistance of Berry Solar Products, Edison, N.J., is gratefully appreciated. Additionally, the authors thank Mr. M. A. Abdallah for assistance in the layout and construction of the window heater.



- | | |
|-------------------------|-------------------------------------|
| Δ THERMOCOUPLE LOCATION | 6. INSULATION |
| 1. INLET | 7. ABSORBER SHEET |
| 2. OUTLET | 8. WINDOW APERTURE INSULATION |
| 3. HINGED WINDOW | 9. FIXTURE HOLDING ANEMOMETER PROBE |
| 4. EXTERIOR WINDOW | 10. WINDOW PANE FRAME |
| 5. PLYWOOD FACING | 11. PASSAGE DIVIDER |

Figure 1 Passive solar window heater

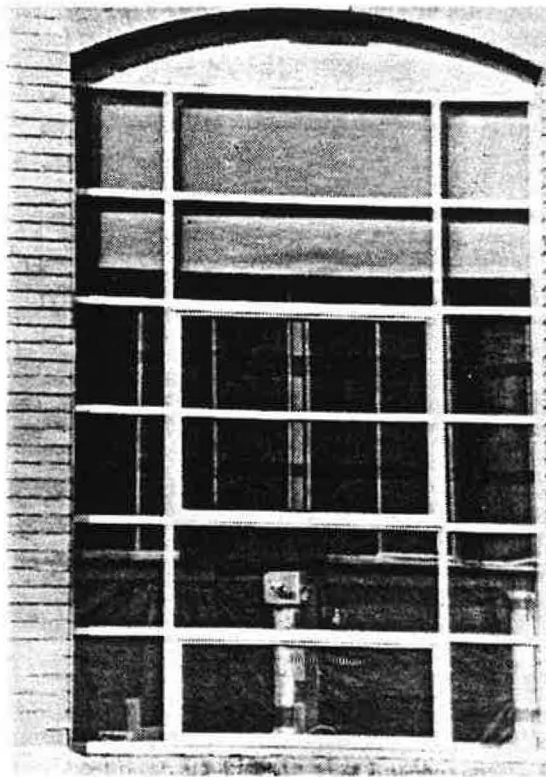


Figure 2 Outside view of window and window heater

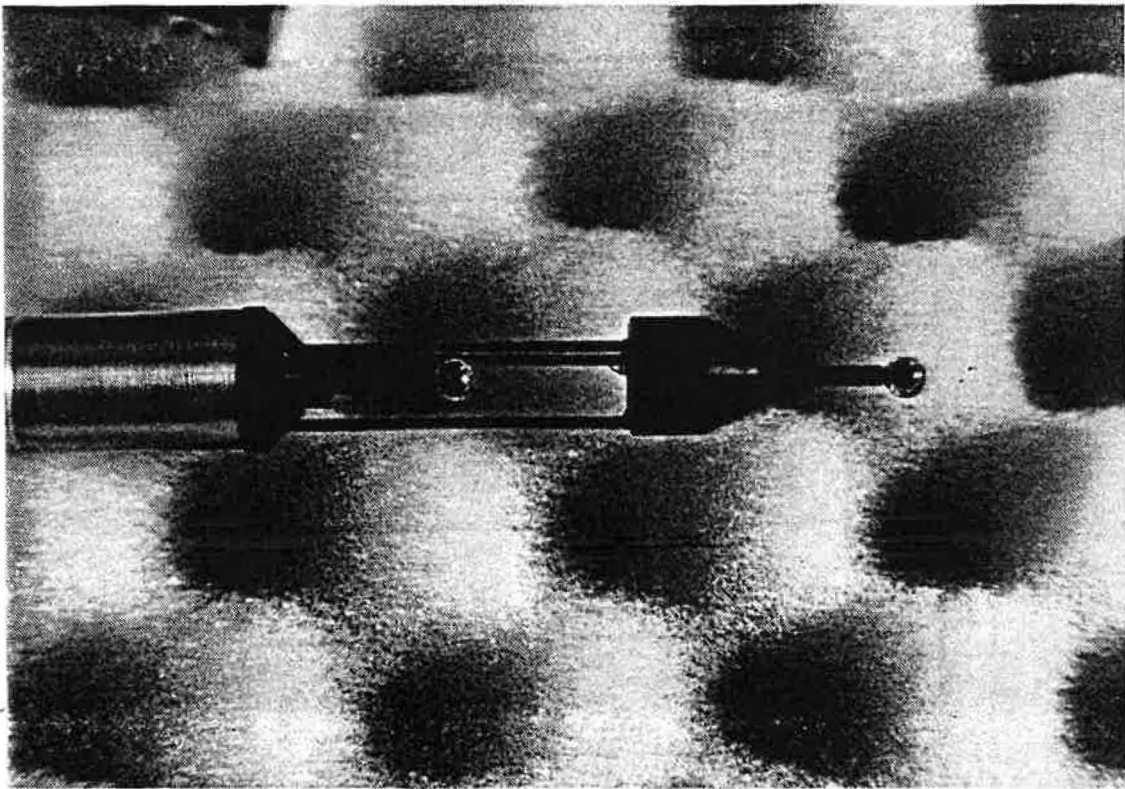


Figure 3 Anemometer probe

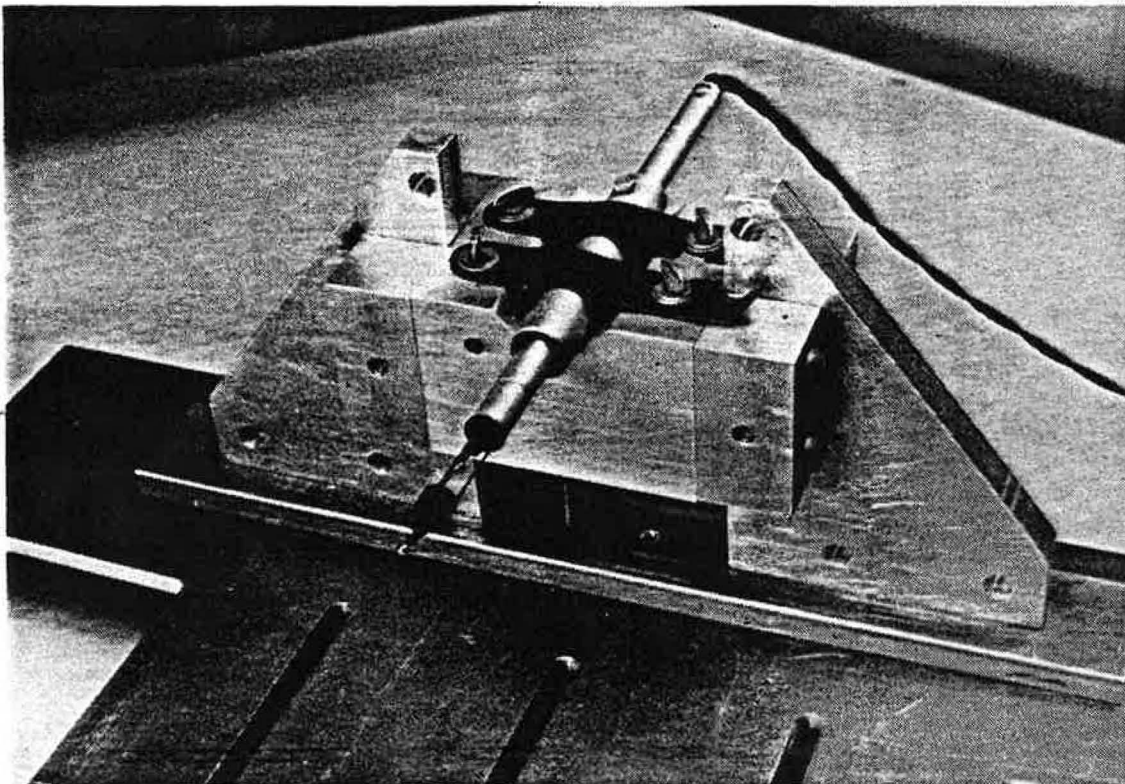


Figure 4 Probe fixture with anemometer probe

TABULATED DATA SETS

Data Sets READING/DIMENSIONS	1	2	3	4	5	6	7	8	9	10	11	12	13
Pyranometer, mV	0.85	1.152	1.956	2.429	2.606	4.977	5.138	5.787	5.868	5.877	5.949	6.231	6.259
Outdoor Temp, °F	82.0	83.0	85.0	88.7	89.8	34.3	14.9	16.4	36.1	38.2	17.3	39.2	37.5
Room Temp, °F	68.8	76.0	74.6	74.9	75.9	75.8	69.1	69.4	78.9	80.1	70.6	80.1	82.3
Flow Out Temp, °F	75.3	81.5	83.7	85.7	88.1	97.3	92.9	94.9	100.5	103.7	97.2	104.9	105.1
Glass Temp, °F	83.2	97.2	102.7	107.2	109.2	74.0	51.6	56.6	82.3	90.7	59.5	92.7	85.3
Anemometer, Volt	3.729	3.951	4.011	4.097	4.101	3.883	3.776	3.804	4.016	4.034	3.839	4.061	4.085
Season	S	S	S	S	S	W	W	W	W	W	W	W	W

Figure 5 Original tabulated data sets

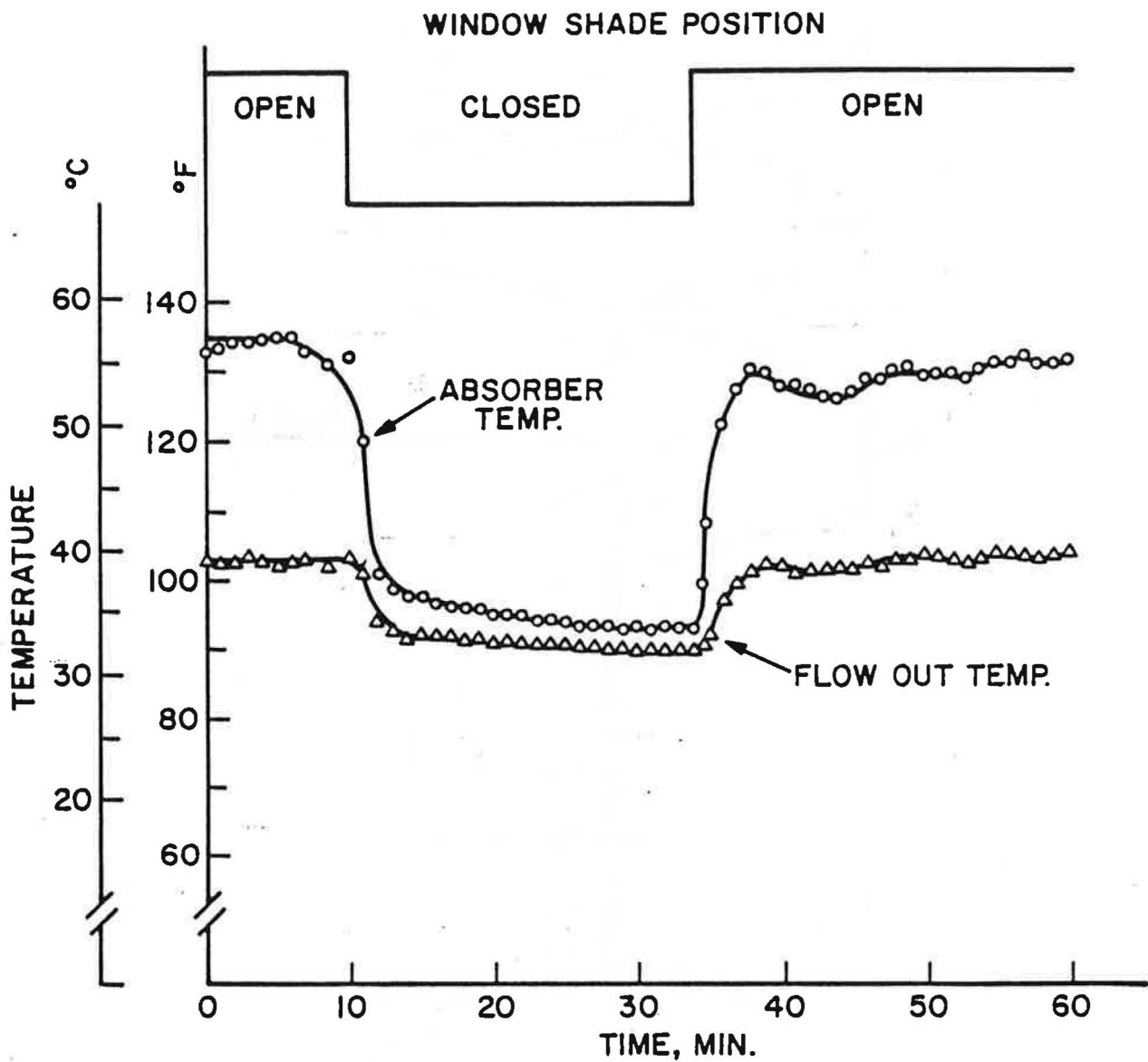


Figure 6 Transient response of window heater

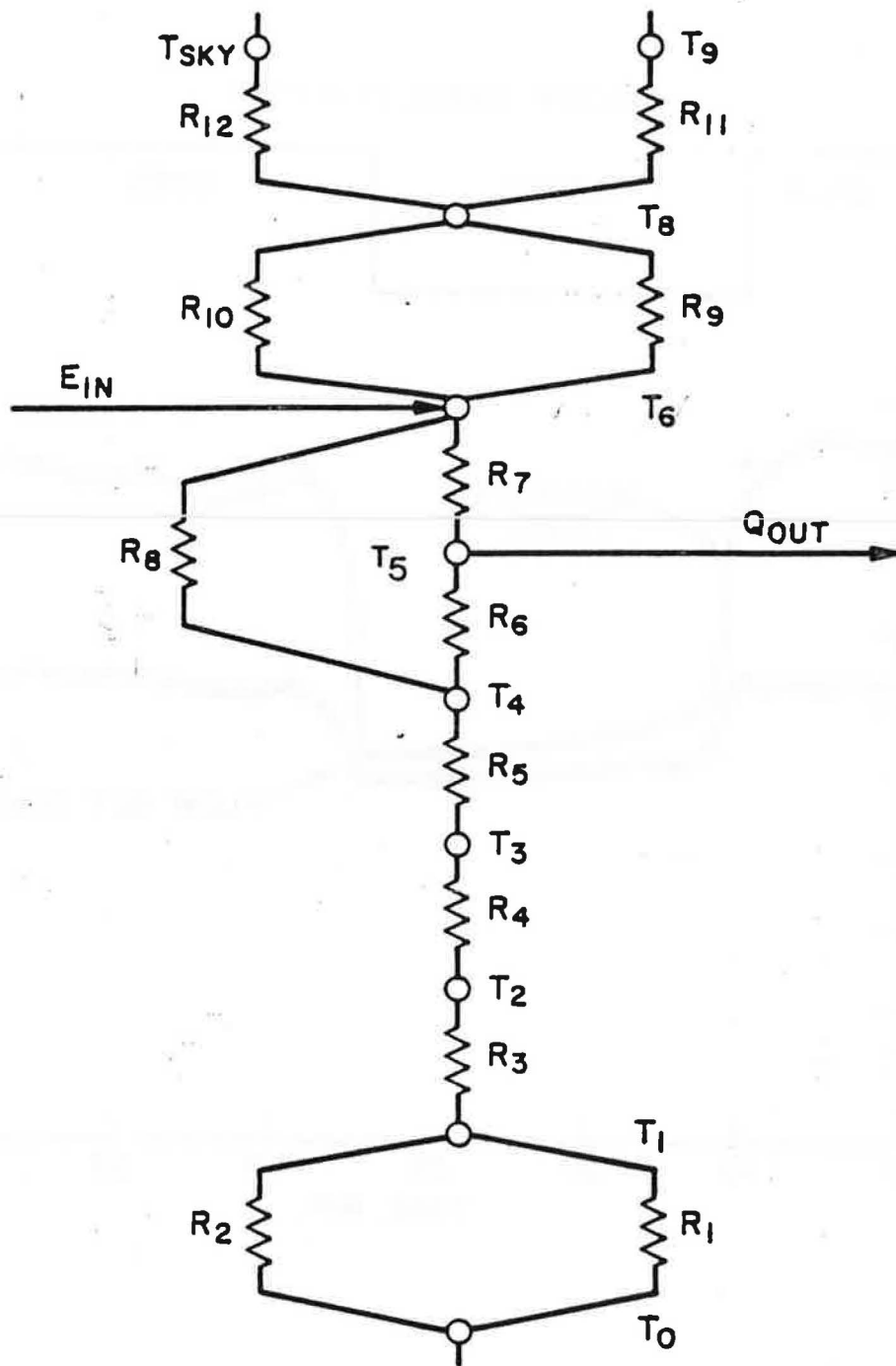


Figure 7 Thermal model for window heater

OUTPUT VS. INSOLATION

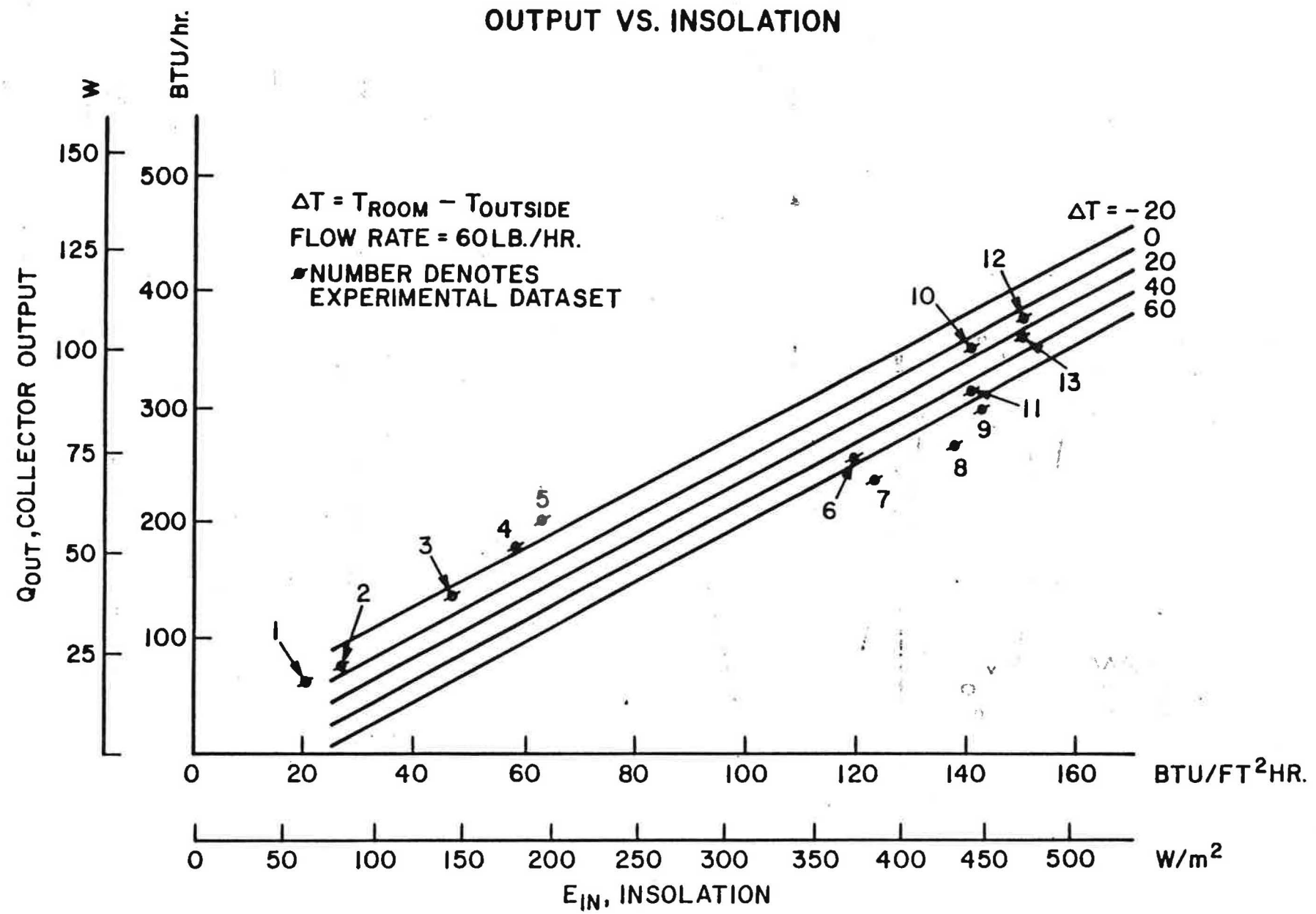


Figure 8 Collector design/performance chart